# Differential Metabolic Sensitivity of mTORC1-and mTORC2-Dependent Overgrowth

Maëlle Devilliers, Damien Garrido, Mickaël Poidevin, Thomas Rubin, Arnaud Le Rouzic, Jacques Montagne

# Differential Metabolic Sensitivity of mTORC1- and mTORC2-Dependent Overgrowth

Maelle Devilliers[1], Damien Garrido[1,‡], Mickael Poidevin[1], Thomas Rubin[1,§], Arnaud Le Rouzic[2], and Jacques Montagne[1,*]

[1] Institute for Integrative Biology of the Cell (I2BC), CNRS, Université Paris-Sud, CEA, F-91190, Gif-sur-Yvette, France

[2] Laboratoire Evolution, Génomes, Comportement et Ecologie, CNRS, Université Paris-Sud, UMR 9191, F-91190, Gif-sur-Yvette, France

* Correspondence: Jacques.MONTAGNE@i2bc.paris-saclay.fr

‡ Present address: IRIC, Université de Montréal, Montréal, Québec H3T 1J4, Canada

§ Present address: Institut Curie, CNRS UMR 3215 / INSERM U-934, F-75248 Paris Cedex 5

Key words: Lipogenesis, Glycolysis, cell-autonomous effect, homeostasis

Short title: Metabolism and mTOR-induced overgrowth

## ABSTRACT

The protein kinase mTOR is implicated in metabolic-related diseases and chiefly controls organismal growth and homeostasis in response to nutrients. Activation of mTOR promotes cell growth and enhances a glycolytic/lipogenic axis, suggesting that this metabolic axis is required to sustain mTOR-dependent growth. Here, we used *Drosophila* genetics to investigate this functional link both at the organismal and cell-autonomous levels. mTOR is present in two distinct complexes mTORC1 and mTORC2, which can be independently modulated in most *Drosophila* tissues. We confirm this independency in the fat body, the organ that fulfils hepatic and adipose functions. We show that ubiquitous mTOR over-activation affects carbohydrate and lipid metabolism, supporting the use of *Drosophila* as a powerful model to study the link between mTOR and metabolism. We show that targeted glycolytic or lipogenic restriction in fat body cells exclusively impedes mTORC2-induced overgrowth. Additionally, ubiquitous deficiency of lipogenesis (*FASN* mutants) results in a drop in mTORC1 but not mTORC2 signaling, whereas, at the cell-autonomous level, lipogenesis deficiency in fat body cells affects neither mTORC1 nor mTORC2 activity. These findings thus, reveal differential metabolic sensitivity of mTORC1- and mTORC2-dependent overgrowth. Furthermore, they suggest that local metabolic defects may elicit compensatory pathways between neighboring cells, whereas enzyme knockdown in the whole organism results in animal death. Importantly, our study weakens the use of single inhibitors to fight mTOR-related diseases and strengthens the use of drug combination and selective tissue-targeting.

## AUTHOR SUMMARY

Cell growth is essential for animal development but is also deregulated in several human diseases including cancers. The mTOR signaling network controls cell growth in response to nutrients and growth factors. mTOR stimulation has been shown to promote basal metabolism, including the glycolytic/lipogenic axis, which is essential to provide energetic cofactors and building blocks to sustain cell growth. However, the requirement this metabolic axis for mTOR-dependent growth has been poorly investigated yet. To address this issue, we used *Drosophila* genetics and focused on the fat tissue that fulfils hepatic and adipose functions. Surprisingly, in mosaic animals, where only a few cells were genetically stimulated for mTOR, we observed that metabolic knockdown only moderates cell overgrowth. Additionally, this growth restriction operates for only one of the two mTOR signaling branches, suggesting that mTOR-dependent compensatory processes operate to circumvent metabolic defects. Given that ubiquitous knockdown of this metabolic axis is essential for juvenile development and adult survival, our study reveals that metabolic restriction is unlikely sufficient to counteract overgrowth disorders.

## INTRODUCTION

Growth of a multicellular organism is coordinated by signaling pathways that adjust intracellular processes to environmental changes. These signaling pathways include the mTOR (mechanistic Target Of Rapamycin) regulatory network that integrates the growth factor response as well as the nutritional and energetic status [1-7]. This network consists in two signaling branches in which the mTOR protein kinase is present in two distinct complexes, mTORC1 and mTORC2 that comprise raptor and rictor, respectively [8, 9]. Both mTORC1 and mTORC2 promote basal cellular functions, thereby providing building blocks to sustain cellular growth. However, despite a plethora of studies on mTORC1/2 signaling and functions, the requirement of basal metabolism—glycolytic/lipogenic axis— for mTOR-dependent cell growth has not been systematically investigated. The *Drosophila* model provides a powerful genetic system to address these issues [10], since both the intermediates of the mTOR signaling network and the basal metabolic pathways are conserved in the fruit fly [11-15].

Regulation of mTORC1 activity by ATP and amino acids depends on a multi-step process that results in the recruitment of an mTORC1 homodimer at the lysosomal membrane in the vicinity of the small GTPase Rheb (Ras homologue enriched in brain) [16-20]. Rheb stimulates mTORC1 activity [21], which in turn regulates several downstream targets. S6Kinase1 (S6K1) is one such kinase, sequentially activated through the phosphorylation of its T389 and T229 residues by mTORC1 and by PDK1 (Phosphoinositide-dependent protein kinase 1), respectively [22, 23]. Further, Rheb activation of mTORC1 is repressed by the tumor suppressor TSC (Tuberous sclerosis complex) that comprises subunits TSC1 and TSC2 [24-27].

The mTORC2 branch resides within the insulin signaling cascade [9]. Binding of insulin or related peptides to their cognate receptors results in recruitment of class I PI3K (Phosphoinositide 3-kinase) to the membrane. PI3K phosphorylates inositol lipids producing phosphatidylinositol-3,4,5-triphosphate (PIP3) [28, 29], while the tumor suppressor PTEN acts as a lipid phosphatase to counteract this process [30]. PIP3 constitutes a membrane docking

site for the protein kinase Akt whose subsequent activation depends on the phosphorylation of its S473 and T308 residues by mTORC2 and PDK1, respectively [31].

Constitutive activation of mTORC1 in MEFs (Mouse embryonic fibroblasts) has been shown to stimulate a metabolic network, including glycolysis, the pentose phosphate pathway and the biosynthesis of fatty acid (FA) and cholesterol [32]. Most of the genes encoding glycolytic enzymes are over-expressed in these cells as are those encoding LDH (lactate dehydrogenase) and Pdk1 (Pyruvate dehydrogenase kinase 1; an inhibitor of mitochondrial pyruvate processing). This suggests that mTORC1-activated MEFs potentiate anaerobic glycolysis and repress the tricarboxylic acid cycle (TCA). Conversely, adipose-specific knockout of raptor to impede mTORC1 formation, results in enhanced uncoupling of mitochondrial activity [33]. The increased lipogenesis observed in mTORC1 stimulated cells depends on a downstream transcriptional regulatory axis involving the cofactor Lipin 1 along with a SREBP (Sterol responsive element binding-protein) family member, which activates genes encoding lipogenic enzymes [32, 34]. Congruently, another study revealed that TSC2 mutant cells become addicted to glucose as a result of mTORC1 hyper-activity [35]. In addition, inhibition of mTORC1 activity revealed that these TSC2 mutant cells become also dependent on glutamine catabolism [36]; mTORC1 potentiates this catabolism to feed TCA anaplerosis, through 1) a S6K/eIF4B/Myc axis that increases glutaminase protein levels [37] and 2) the repression of SIRT4, a mitochondrial sirtuin that inhibits glutamine dehydrogenase [38].

Besides mTORC1 mediated regulation, mTORC2 also impinges on basal metabolism. Intracellular activation of Akt increases ATP levels [39, 40] through the stimulation of GLUT4-mediated glucose uptake [41] and the enhancement of the expression and activity of glycolytic enzymes [42, 43]. Akt also dampens glucose production by suppressing PEPCK (gluconeogenesis), glucose-6-phosphatase (glycogenolyse) and the glycogen synthesis repressor GSK3 [44, 45]. However, in contrast to mTORC1, Akt also promotes mitochondrial metabolism and oxidative phosphorylations [42, 46]. Conversely, hepatic knockout of the mTORC2 specific-subunit rictor results in constitutive gluconeogenesis and impaired glycolysis

and lipogenesis [47, 48]. Taken together, these studies strongly emphasize the role of mTOR in metabolic-related diseases and in adjusting metabolism to the nutritional and energetic status [7].

In the present study, we investigated the requirement of the glycolytic/lipogenic axis for the cellular growth induced by mTORC1 and mTORC2 hyper-activation in *Drosophila*. As previously demonstrated mTORC1 and mTORC2 reside on independent signaling branches in most *Drosophila* tissues [24, 49-52]. Here, we confirmed mTORC1 and 2 independency in the fat body (FB), the organ that fulfils hepatic and adipose functions to control body homeostasis in *Drosophila* [12, 13, 15]. We analyzed the effect of ubiquitous mTOR activation on glycolysis and lipogenesis. We show that in increase in mTOR activity provokes an apparent enhancement of metabolite consumption. Furthermore, our study reveals that metabolic restriction at the organismal level has dramatic consequences on animal survival, but no effect at the cell-autonomous level, suggesting that within an organism, alternative pathways may operate to compensate local metabolic defects. Nonetheless, at the cell-autonomous level, metabolic restriction can restrain mTORC2- but not mTORC1-induced overgrowth, indicating that the potential compensatory metabolic pathways do not fully operate in the context of mTORC2 over-activation.

## RESULTS

### mTORC1 and mTORC2 independency in the fat body

Previous studies showed that mTORC1 and mTORC2 reside on independent signaling branches in most *Drosophila* tissues [24, 49-52]. Activating either the mTORC1 or the mTORC2 signaling branch can be performed by overexpressing Rheb or depleting PTEN, respectively. To investigate mTORC1/2 independency in the FB, we generated somatic clones either over-expressing Rheb (*Rheb*$^{+}$) [53] or homozygote for a *PTEN* mutation (*PTEN*$^{-/-}$) [54]. The precursors of FB cells divide in the embryo; during larval life, the differentiated cells do not

divide but endoreplicate their DNA content to reach a giant size [55]. Therefore, to precisely evaluate the effect on cell growth, somatic recombination events were induced during embryogenesis at the stage of proliferation of the FB cell precursors and the resulting MARCM clones were analyzed in the FB of late feeding L3 larvae, prior to the wandering stage that precedes metamorphosis entry. Both *PTEN*$^{-/-}$ and *Rheb*$^{+}$ clonal cells were bigger than the surrounding control cells and this cell size effect was dramatically increased in *PTEN*$^{-/-}$;*Rheb*$^{+}$ combined clones (Figure 1A-D and 1M). We next analyzed this growth increase in the context of the previously described *mTOR*$^{2L1}$ and *mTOR*$^{\Delta P}$ mutations. However, we could not find mutant clones in the FB. Consistent with previous studies reporting that mTOR is critically required for cell growth of endoreplicative tissues [54, 56], we reasoned that these clonal cells were likely eliminated by cell competition [57]. Thus, we generated somatic clones in a *Minute* background to slow down the growth of the surrounding control cells. In these conditions, *mTOR* mutant clones could indeed be recovered. Both *mTOR*$^{2L1}$ and *mTOR*$^{\Delta P}$ mutant cells exhibited a dramatic size reduction (Figure 1G and 1J) and this phenotype was dominant in *Rheb*$^{+}$ combined clonal cells (compare Figure 1E to 1H and 1K). In contrast, *mTOR*$^{\Delta P}$ but not *mTOR*$^{2L1}$ exhibited a clear dominant phenotype over the *PTEN*$^{-/-}$ mutation; the size of *mTOR*$^{\Delta P}$,*PTEN*$^{-/-}$ clonal cells was dramatically reduced, whereas *mTOR*$^{2L1}$,*PTEN*$^{-/-}$ clonal cells were giant (compare Figure 1F to 1I and 1L). These findings indicate that the *mTOR*$^{2L1}$ mutation affects mTORC1 but not mTORC2 signaling, whereas *mTOR*$^{\Delta P}$ affects both signaling branches.

Next, we used phospho-specific antibodies in immunostaining assays to analyze the phosphorylation of Akt (P-Akt) and of the dS6K target, ribosomal protein rpS6 (P-S6). In *PTEN*$^{-/-}$ clonal cells, we observed an increase in the P-Akt intracellular signal (Figure 2A). Importantly the P-Akt intracellular signal was absent in *mTOR*$^{\Delta P}$ cells (Figure 2B) but not affected in *mTOR*$^{2L1}$ cells (Figure 2C). Staining with the rpS6 phospho-specific antibody revealed a patchy signal, with only a subset of cells expressing the P-S6 signal in the FB (Figure 2E-J), a pattern previously described in the wing imaginal disc [58]. Therefore, to evaluate mTORC1 activity, we measured the ratio of P-S6 positive cells among the population of GFP$^{+}$ clonal cells. For control

clones, only labeled by GFP, about half of them were P-S6 positive (Figure 2E and 2K), whereas most of the *mTOR*$^{2L1}$ and *mTOR*$^{\Delta P}$ clones were P-S6 negative (Figure 2F, 2G and 2K). Importantly, almost all the *Rheb*$^{+}$ cells were P-S6 positive (Figure 2H and 2K), whereas the ratio of P-S6 positive cells was slightly but not significantly increased in the *PTEN*$^{-/-}$ cell population (Figure 2I and 2K). Taken together, these findings confirm that mTORC1 and mTORC2 operate independently in FB cells and reveal that the *mTOR*$^{2L1}$ mutation affects only mTORC1, whereas the *mTOR*$^{\Delta P}$ mutation affects both signaling branches.

**Activating mTORC1 or mTORC2 signaling impacts basal metabolism**

A number of studies support the notion that mTOR activity controls metabolism to sustain cellular growth. To evaluate how mTORC1 and mTORC2 affect basal metabolism in *Drosophila*, we analyzed various metabolites in whole animals that express the ubiquitous *da-gal4* driver to direct Rheb overexpression (*Rheb*$^{++}$) or PTEN knockdown by RNA interference (*PTEN-RNAi*). Larvae were fed either a standard or a 20%-sucrose supplemented diet (20%-SSD) and 0-5h prepupae were collected, as this is a convenient phase to stage the animals after the feeding period. When fed a standard diet, a high rate of lethality was observed for *Rheb*$^{++}$ and *PTEN-RNAi* larvae, although a sufficient number of prepupae could be collected for metabolic analysis. In contrast, none of the *Rheb*$^{++}$ and *PTEN-RNAi* larvae reached the prepupal stage when fed a 20%-SSD. Nonetheless, when *Rheb*$^{++}$ and *PTEN-RNAi* larvae were fed a standard diet during early larval life and transferred onto a 20%-SSD at the L2/L3 molting transition, we could recover a few prepupae for metabolic measurements. For both males and females fed a standard diet, the body weight of *Rheb*$^{++}$ and *PTEN-RNAi* prepupae was roughly similar to that of controls (Figure 3A and 3B). Conversely, providing a 20%-SSD resulted in a drop of the prepupal weight of control animals that was significantly compensated in *Rheb*$^{++}$ and *PTEN-RNAi* prepupae (Figure 3A and 3B).

Next, we measured the total amounts of protein, triacylglycerol (TAG), glycogen and trehalose—the most abundant circulating sugar in *Drosophila*. Although variations in protein levels were

observed, none of them were statistically significant (Figure 3C). TAG levels in control prepupae were not affected by sucrose supplementation and did not vary in *PTEN-RNAi*, but were significantly decreased in *Rheb*$^{++}$ animals (Figure 3D). Feeding larvae a 20%-SSD since the L2/L3 molting transition resulted in a marked in increase in glycogen and trehalose levels in control prepupae (Figure 3E-F). In *Rheb*$^{++}$ and, in lower extent, in *PTEN-RNAi* prepupae, glycogen levels were significantly lower than those measured in controls (Figure 3E). Finally, trehalose levels were strongly decreased in both *Rheb*$^{++}$ and *PTEN-RNAi* prepupae fed either a standard or a 20%-SSD as compared to the control (Figure 3F). Taken together, these findings suggest that a ubiquitous increased activity of either mTORC1 or mTORC2 provokes an apparent increase in metabolite consumption. This metabolic rate is correlated with a relative increase in body weight for larvae fed a 20%-SSD, but not for those fed a standard diet. We previously observed that increasing dietary sucrose induced a reduction in food intake [59] that may account for the body weight reduction of control animals. Potentially, food intake could be less affected in *Rheb*$^{++}$ and *PTEN-RNAi* animals, thereby leading to a compensatory effect on body weight. Measuring food intake in *Rheb*$^{++}$ or *PTEN-RNAi* larvae was not applicable since most of them die during larval stage and thus, terminate feeding earlier. In sum, our data indicates that basal metabolism is altered in the few *Rheb*$^{++}$ or *PTEN-RNAi* larvae that survive and further suggests that in most cases stronger metabolic disruption happened, resulting in lethal homeostatic defects.

**Knocking-down glycolysis at the whole body level**

Since manipulating mTOR resulted in a decrease in the levels of TAG and glycogen stores and of circulating trehalose (Figure 3), we asked whether the basal energetic metabolism affected mTOR signaling. First, we ubiquitously expressed interfering RNA against phosphofructokinase1 (*PFK1-RNAi*), pyruvate kinase (*PK-RNAi*) pyruvate dehydrogenase (*PDH-RNAi*) and lactate dehydrogenase (*LDH-RNAi*). PFK1 catalyzes the third glycolytic reaction to form fructose 1,6-bisphophate; PK catalyzes the final glycolytic reaction to form

pyruvate; PDH directs the mitochondrial fate of pyruvate, whereas LDH directs its anaerobic fate (Figure 4A). When directed with the ubiquitous *da-gal4* driver, *PK-RNAi* provoked early larval lethality, *PFK1-RNAi* and *PDH-RNAi* provoked larval lethality at L2 or L3 stages, whereas *LDH-RNAi* induced a semi-lethal phenotype at larval or pupal stages (Figure 4B).

Second, to monitor mTOR activity following ubiquitous knockdown of glycolysis, the *da-gal4* driver was combined with a ubiquitous thermo-sensitive form of the Gal4 inhibitor, Gal80$^{ts}$ (*tub-gal80$^{ts}$*) that blocks Gal4 activity at 21°C but not at 29°C, thereby allowing RNAi expression after temperature shift. Each RNAi was ubiquitously induced at early L1 stage and protein extracts were prepared two days later using late L2 larvae. At this stage the larvae were still viable, although those expressing PK-RNAi did not undergo L2/L3 transition and eventually died (Figure 4B). Western-blotting using these L2 protein extracts revealed that RNAi-knockdown of PFK1, LDH or PDH did not affect Akt or dS6K phosphorylation (Figure 4C). In contrast, PK knockdown strongly decreased dS6K phosphorylation and to a lower extent Akt phosphorylation (Figure 4C). These results indicate that mTORC1 signaling may be affected when knocking down PK, but not when knocking down any other enzyme directly linked to glycolysis. Nonetheless, the lethal phenotype of PK-RNAi larvae occurring at the late L2 stage (Figure 4B) might weaken the larvae, inducing a subsequent effect on mTOR signaling.

To evaluate the requirement of glycolysis for adult survival, RNAi-knockdown was induced by temperature shift to 29°C in newly emerged flies and lethality was counted every second day. In both males and females, PK and PFK1 knockdown provoked lethality between 10 to 14 days after temperature shift (Figure 4D). Knockdown of PDH and LDH also induced adult lethality, although not as soon as PK and PFK1 knockdown (Figure 4D). As a comparison, we analyzed FASN knockdown in adults; about a quarter of *FASN-RNAi* flies died between 10 to 14 days, while the others survived nearly as well as control flies (Figure 4D). Taken together, these data indicate that glycolysis is essential for both larval development and adult survival. However, prior to the appearance of the deleterious phenotype, glycolysis knockdown is unlikely to impinge on mTOR signaling.

246

247 **Cell-autonomous requirement of glycolysis for mTORC2- but not mTORC1-dependent**
248 **overgrowth**

249 To investigate the requirement of glycolysis to sustain mTOR-dependent growth at the cell-
250 autonomous level, *PFK1-RNAi*, *PK-RNAi*, *PDH-RNAi* and *LDH-RNAi* were induced in *PTEN*$^{-/-}$ or
251 *Rheb*$^{+}$ clones. Except a moderate effect of *PK-RNAi*, clones expressing interfering RNA against
252 these metabolic enzymes did not significantly affect the growth of FB cells (Figure 5A-D and
253 5M). In combined clones, none of the RNAi affected the growth of *Rheb*$^{+}$ clones (Figure 5E-H
254 and 5M). In contrast, the size of *PTEN*$^{-/-}$ clones was significantly decreased when co-expressing
255 RNA against any of these metabolic enzymes (Figure 5I-M). These findings indicate that both
256 aerobic and anaerobic glycolysis are required to sustain mTORC2-dependent overgrowth at the
257 cell-autonomous level. In contrast, reducing glycolysis does not counteract mTORC1-dependent
258 overgrowth, suggesting the existence of compensatory pathways.

259

260 **Effect of Lipogenesis on mTOR signaling**

261 Since glycolysis and FA synthesis are tightly connected metabolic pathways [59], we
262 investigated whether lipogenesis affects mTOR signaling. FA synthesis is catalyzed by FASN
263 (Figure 4A). The *Drosophila* genome encodes three *FASN* genes, *FASN1* is ubiquitously
264 expressed but not *FASN2* or *FASN3* [60-62]. The deletion of the *FASN1* and *FASN2* tandem
265 (*FASN*$^{\Delta 24\text{-}23}$ deletion, hereafter called *FASN*$^{1\text{-}2}$) results in a lethal phenotype that can be rescued
266 by feeding larvae a lipid-complemented diet (beySD) [59, 62]. We observed that beySD-rescued
267 *FASN*$^{1\text{-}2}$ mutant larvae exhibited a delay in development, as measured by the duration of larval
268 development to metamorphosis entry (Figure 6A). Further, when beySD-rescued *FASN*$^{1\text{-}2}$
269 mutant larvae were transferred at the L2/L3 larval transition onto a 10% sucrose-supplemented-
270 beySD, only a few of them completed the third larval stage and, after an extreme developmental
271 delay, entered metamorphosis (Figure 6A). Delay in development can be due to a default in

ecdysone production that results in giant pupae [63] or to impaired mTOR signaling that results in reduced body growth [54, 64]. Measurements of prepupal weight revealed that *FASN*$^{1-2}$ mutant prepupae exhibited a severe reduction in body weight, whether or not they were supplemented with sucrose (Figure 6B), suggesting a default in mTOR signaling. Therefore, we analyzed the phosphorylation of the *Drosophila* S6Kinase (dS6K) and Akt in protein extracts of late feeding L3 larvae. Western-blotting revealed that the dS6K protein resolved in several bands in *FASN*$^{1-2}$ extracts, whereas Akt protein was unchanged (Figure 6C). These results suggest that dS6K but not Akt might be degraded in the *FASN*$^{1-2}$ mutant background. In addition, dS6K phosphorylation decreased in *FASN*$^{1-2}$ extracts and became barely detectable when *FASN*$^{1-2}$ larvae were fed a sucrose-supplemented-beySD (Figure 6C). Conversely, the phosphorylation of Akt was unaffected in larvae fed a beySD, although it was slightly decreased in larvae fed a sucrose-supplemented-beySD (Figure 6C). This finding contrasts with our previous observation showing that FB explants of *FASN*$^{1-2}$ mutant larvae were hypersensitive to insulin [59]. However, *FASN*$^{1-2}$ mutants also exhibited a decrease in food intake [59], which might induce a systemic suppression of dS6K phosphorylation, while FB explant were cultured in nutrient media supplemented with insulin. Therefore, to determine whether *FASN* mutation affects mTOR signaling at the cell-autonomous level, we analyzed P-S6 and P-Akt in *FASN*$^{1-2}$ mutant clones in the FB. As for control clones, about half of the *FASN*$^{1-2}$ clonal cells were P-S6 positive (Figure 2J and 2K). Furthermore, no effect on P-Akt was observed in *FASN*$^{1-2}$ clonal cells (Figure 2D). In summary, these findings reveal that disrupting FA synthesis does not significantly affect mTORC1 and mTORC2 signaling at the cell-autonomous level, although it seems to impinge on mTORC1 signaling when inhibited in the whole animal whether directly or indirectly.

**Cell-autonomous requirement of FA synthesis for mTORC2- but not mTORC1-dependent overgrowth**

To determine, whether lipogenesis is required at the cell-autonomous level to sustain mTORC1 and/or mTORC2 dependent growth, we analyzed *FASN*$^{1-2}$ clones while enhancing either of the mTOR signaling branch in FB cells. We previously reported [59] that *FASN*$^{1-2}$ clonal cells in the FB were slightly reduced in size and that this effect was dramatically increased in larvae fed a 20%-SSD (Supplementary Figure S1 and Figure 7M). Therefore, we generated *PTEN*$^{-/-}$ and *Rheb*$^{+}$ clones combined or not with the *FASN*$^{1-2}$ mutation and analyzed them in the FB of larvae fed either a standard diet or a 20%-SSD. As compared to the standard diet, feeding larvae a 20%-SSD had no effect on the size of *Rheb*$^{+}$ clonal cells, but significantly reduced the size of *PTEN*$^{-/-}$ and of *PTEN*$^{-/-}$;*Rheb*$^{+}$ clonal cells (Figure 7A-F and 7M). Further, when combined with the *FASN*$^{1-2}$ mutation, *PTEN*$^{-/-}$ but not *Rheb*$^{+}$ clones were significantly reduced in size (Figure 7G-H and 7M). The *FASN*$^{1-2}$ mutation also provoked a severe size reduction of *PTEN*$^{-/-}$,*Rheb*$^{+}$ clones (Figure 7I and 7M). Moreover, as compared to the standard diet, feeding larvae a 20%-SSD induced a significant size reduction of *FASN*$^{1-2}$;*Rheb*$^{+}$, *FASN*$^{1-2}$,*PTEN*$^{-/-}$ and *FASN*$^{1-2}$,*PTEN*$^{-/-}$;*Rheb*$^{+}$ clonal cells (Figure 7J-L and 7M). Of note, except for the *FASN*$^{1-2}$;*Rheb*$^{+}$ clonal cells in larvae fed a 20%-SSD that exhibited a size roughly identical to that of the surrounding control cells (Figure 7J), the cell size was always bigger than the controls (Figure 7M). These findings indicate that, in larvae fed a standard diet, FA synthesis is at least in part required to sustain over-growth induced by mTORC2, but not mTORC1. They also reveal that additional dietary sucrose is rather detrimental for the growth of cells either deficient for FA synthesis or over-active for mTORC2, suggesting that these cells have a restricted homeostatic ability to adjust to an unbalanced diet, whereas mTORC1 activated cells at least in part maintain this ability.

## DISCUSSION

In this study, we used the powerful *Drosophila* genetics to investigate the functional links between mTOR-dependent growth and the glycolytic/lipogenic axis. On one hand, we dampened this metabolic axis or enhanced mTORC1/2 activity in the whole organism to mimic the effect that might be induced by drug treatment with a systemic inhibitor. On the other hand,

to monitor the cell growth process that spans the entire developmental program at the cell-autonomous level, we analyzed clonal FB cells in mosaic animals. Intriguingly, our study reveals apparent contradictory effects between perturbations at the whole body and cell-autonomous levels.

At the organismal level, knockdown of glycolytic enzymes or deficiency of FASN result in animal lethality. However, *FASN*$^{1-2}$ mutant animals supplemented with dietary lipids can survive but exhibit a dramatic overall growth suppression. This growth defect might result from a decrease in mTORC1 activity that is strongly reduced in *FASN*$^{1-2}$ mutant animals, suggesting that mTORC1 but not mTORC2 signaling relies on lipogenesis. In contrast, at the cell autonomous level, the mutation of *FASN*$^{1-2}$ restrains mTORC2 but not mTORC1 dependent overgrowth in FB cells. These apparent contradictory findings, suggest that the growth defect and the reduction of mTORC1 activity in *FASN*$^{1-2}$ mutants are not due to the addition of cell-autonomous effects but rather to a systemic regulation. Potentially, FASN default might affect the activity of a specific tissue, as for instance, the neurosecretory cells that synthesize and secrete insulin like peptides, which promote systemic body growth [65]. Alternatively, considering that mTORC1 directly responds to nutrients [18-20], the drop of mTORC1 activity may be a consequence of feeding, since we previously reported a decrease in nutrient uptake in *FASN*$^{1-2}$ mutant animals [59]. Consistently, a previous study on the transcription factor mio —the *Drosophila* homologue of mondoA and ChREBP that regulate the glycolytic/lipogenic axis in response to dietary sugar [66, 67]— suggests the existence of a FASN-dependent effect in the FB on the control of food intake [68]. FB-knockdown of *mio* results in the lack of sucrose-induced expression of *FASN1* and in a decrease in food intake. This study suggests that the FASN default perturbs body homeostasis and indirectly affects the neuronal control of feeding behavior. However, it does not exclude that a lipogenic defect in neuronal cells may also directly impinge on feeding behavior. Finally, the drop of mTORC1 activity observed in *FASN*$^{1-2}$ mutants may be a consequence of malonyl-CoA accumulation, since mTOR malonylation has been reported to inhibit mTORC1 but not mTORC2 activity [69]. Malonylation of mTOR may also account for the

size reduction of *FASN*$^{1-2}$ mutant cells over-expressing Rheb in animals fed a 20%-SSD, consistent with the increased expression of lipogenic enzymes induced by dietary sucrose [59]. Thus, mTOR malonylation and the subsequent decrease in mTORC1 activity might occur only when interfering with a context of high demand for lipogenesis.

Our study reveals that over-activation of mTORC1 and to a lesser extent of mTORC2, results in a decrease in glycogen and TAG stores and in circulating trehalose, suggesting that mTOR activation enhances metabolite consumption to sustain cell growth. It is therefore surprising that activation of neither mTORC1 nor mTORC2 induces an increase in body weight. Nonetheless, overall body growth depends on an intricate regulatory network that integrates cell-autonomous effects and humoral messages. For instance, previous studies reported that mTOR activation within the ring gland, results in a systemic decrease in body growth [70-72]. Therefore, mTOR ubiquitous activation is likely to promote the growth of most cells but might concurrently perturb endocrine signals dampening overall growth. Of note, we observed that larvae fed a 20%-SSD result in pupae with reduced body weight, an effect that is partially suppressed when either of the mTORC-signaling branch is over-activated. The fact that the overall body weight of mTOR-stimulated animals is maintained within a range likely compatible with organismal survival contrasts with the observed high rate of lethality. The decrease in stores and circulating sugars suggests that in these animals each cell tends to increase its basal metabolism evoking an egoist behavior that might perturb the equilibrium between cell-autonomous and systemic regulation. Thus, in a stressful situation, as when animals are fed a 20%-SSD, the need of a tight adjustment to an unbalanced diet may enhance the distortion between cell-autonomous effects and systemic regulation, resulting in an increased rate of lethality.

In agreement with other studies [24, 49-52], we show that the mTORC1 and mTORC2 branches work independently in the *Drosophila* FB and we provide evidence that the previously described *mTOR*$^{2L1}$ mutation [54] affects mTORC1 signaling only. A plethora of studies in mammalian cells indicate that mTOR activation directs metabolism towards glucose consumption, storage and anabolism [32, 34, 35, 39, 41-43, 73]. Our study rather suggests that in the *Drosophila*

larvae, mTOR promotes metabolite consumption through glycolysis but not storage. However, at the cell-autonomous level, we observe that inhibition of lipogenesis or glycolysis restrains neither larval FB cell growth nor overgrowth induced by mTORC1 stimulation in these cells. These findings counteract the idea that mTORC1 potentiates a glycolytic/lipogenic axis [32] to sustain cell growth. To overcome the lack of glycolytic products and of membrane lipids, these cells may benefit of a transfer from neighboring cells and might favor alternative metabolic pathways, including glutamine catabolism to feed TCA anaplerosis which has been shown to be a crucial pathway in mTORC1-stimulated mammalian cells [36-38]. Nonetheless, such compensatory processes do not fully operate to sustain mTORC2-dependent overgrowth. In these cells, the mutation of PTEN results in mTORC2 hyper-activation and potentially impedes the ability to modulate this signaling branch. Therefore, it is tempting to speculate that the modulation of mTORC2 signaling at least in part contributes to the regulation of these compensatory processes.

As a coordinator of growth and metabolism, mTOR plays a central role in tumor development [7, 74, 75]. PTEN, the tumor suppressor that counteracts PI3K activity upstream of mTORC2 signaling, is deficient in several human cancers [30]. Mutation of TSC1 or TSC2, the essential subunits of the tuberous sclerosis complex, is associated with benign tumors but also with brain, kidney and lung destructive diseases [76]. To investigate the role of mTOR regarding tumor development, a recent study reported the generation of liver-specific double knockout mice for TSC1 and PTEN [77]. These mice develop hepatic steatosis that eventually progresses to hepatocellular carcinoma. Both processes are suppressed in mice fed the mTORC1/2 inhibitors INK128, but not the mTORC1 inhibitor rapamycin, supporting an mTORC2 specific effect. The combination of inhibitors against mTOR and metabolism is currently under clinical investigation to fight cancers [7]. Importantly, our study reveals that ubiquitous inhibition of basal metabolism produces dramatic effects during development, while it only moderates cell growth induced by mTOR over-activation. Therefore, the use of drug therapy to fight cancer must be taken with

405 caution, in particular if development is not complete and most efforts should be made to
406 selectively target sick tissues.

407

408 **MATERIAL & METHODS**

409 **Genetics and fly handling**

410 Fly strains: *P[w[+mC]=tubP-GAL80]LL10,P[ry[+t7.2]=neoFRT]40A*, *daughterless(da)-gal4*, *tub-*
411 *gal80$^{ts}$*, *UAS-Dcr-2* (Bloomington Stock Center); *FASN$^{1-2}$* [59]; *mTOR$^{\Delta P}$* [56]; *mTOR$^{2L1}$* and
412 *PTEN* [54]; *EP(UAS)-Rheb* [53]; ); inducible RNA-interfering (*UAS-RNAi*) lines to *PTEN* (NIG
413 5671R-2), *FASN1* (VDRC 29349), *PFK1* (VDRC 3017), *PK* (VDRC 49533) *PDH* (VDRC 40410),
414 *LDH* (VDRC 31192) [78]. The *Minute* stock used was previously referred to as *FRT40/P(arm-*
415 *LacZ w$^{+}$)* [79] but exhibit both developmental delay and short and slender bristles, typically
416 reported as *Minute* phenotype [57]. To generate MARCM clones in the *Minute* background,
417 these flies were recombined with the *P[w[+mC]=tubP-GAL80]LL10,P[ry[+t7.2]=neoFRT]40A*
418 chromosome.

419 The standard media used in this study contained agar (1g), polenta (6g) and yeast (4g) for
420 100ml. Lipid- (beySD) and sugar-complemented media were prepared as previously described
421 [59].

422 To select *FASN$^{1-2}$* mutant larvae, we used a GFP-labelled CyO balancer chromosome. Flies
423 were let to lay eggs on grape juice plates for less than 24 hrs. Then, some beySD media was
424 put in the middle of the plates; larvae that do not express GFP were collected the next day and
425 transferred to fresh tubes. Prepupae were collected once a day to evaluate developmental delay
426 and to measure body weight.

427

428 **Molecular biology and Biochemistry**

429 To test RNAi-knockdown efficacy to the glycolytic enzymes (Supplementary Figure S2), *UAS-*
430 *Dcr-2;da-gal4,tub-gal80$^{ts}$* virgin females were mated with UAS-RNAi males. Flies were let to lay

eggs overnight and tubes were kept at 19°C for two days. Tubes were then transferred at 29°C and two days later, larvae of roughly the same size were collected. Reverse transcription and quantitative PCR were performed as previously described [60].

Protein extracts for western-blotting were prepared as previously described [51]. Antibody used in for western-blotting have been previously described [51] or commercially provided for Akt (Cell signaling 4054).

For metabolic measurements, parental flies were let to lay eggs in tubes for less than 24 hrs at 25°C. Tubes were then transferred at 29°C to strengthen the gal4/UAS effect, and using a *UAS-Dcr-2* to strengthen the RNAi effect. Larvae were either maintained in the same tubes or selected prior to L2/L3 transition and transferred on 20%-SSD. Collection of prepupae and metabolic measurements were performed as previously described [59].

**Clonal analysis**

All the clones were generated using the MARCM strategy [80]. Parental flies were let to lay eggs at 25°C for seven hrs. Tubes were then heat shocked for 65 minutes in a water bath at 38°C so that recombination happens while FB precursor cells are in dividing process. FB from feeding larvae at the end of the L3 stage where dissected, fixed, membranes were labelled with phalloidin and nuclei with DAPI, and FB were mounted as previously described [59]. Image acquisitions were obtained using a Leica SP8 confocal laser-scanning microscope. For immuno staining the phospho-S6 antibody has been previously described [58] and the phospho-Akt commercially provided (Cell signaling 4054). The cell size calculation have been performed as previously described [59] and correspond to a set of experiments that spanned a two-year period. It represent too many replicates, so that it was not possible to make them at the same time. Therefore, for the graphs of cell size measurement (Figure 2M, 5M and 6G), values are reused when they correspond to the same genotype and conditions. This allows a direct comparison between the experiments.

## Statistical analysis

Statistical analyses were performed with R version 3.4.4, scripts are available on request. Significance for the statistical tests was coded in the following way based on the p-values: ***: 0 < p < 0.001; **: 0.001 < p < 0.01; *: 0.01 < p < 0.05. P-values were corrected for multiple testing by a Holm-Bonferroni method [81]. Clone sizes were analyzed with a mixed-effect linear model on the logarithm of cell area, considering the treatment (Genotype and Sucrose conditions) as a fixed effect and Series/Larva as random effects (Figures 1, 5, and 7, Supplementary Table S1). The reported effects (and the corresponding P-values) were obtained from the difference between the (log) area of marked clonal cells and that of control surrounding cells from the same treatment, by setting the appropriate contrast with the "multcomp" package [82], according to the pattern: EA,B = log(MA) – log(WA) – [log(MB) – log(WB)], where EA,B is the difference between treatments (genotype and sucrose levels) A and B, MA and MB standing for the area of marked cells, and WA, WB for the area of control cells in those treatments. This is equivalent to testing whether marked/control cell area ratios differ between treatments. PS6+ clone frequencies were treated as binomial measurements in a mixed-effect generalized linear model "lme4" package [83], featuring Genotype as a fixed effect, and Series/Larva as random effects. Both datasets of pupal weights were analyzed independently with linear models including Sex, Genotype, and Sucrose level effects and all their interaction terms (Figure 3A-B and Supplementary Table S3 for PTEN knockdown and Rheb overexpression; and Figure 6B and Supplementary Table S4 for *FASN*$^{1-2}$ mutants). TAG, Protein, Glycogen, and Threalose concentrations were also analyzed with linear models involving Genotype, Sucrose level, and their interactions as fixed effects (Fig3 and Supplementary Table S3).

## AKNOWLEDGMENTS

We wish to thank D Petit for preparing the fly media, H Stocker for fly stocks, A Teleman for the phospho-S6 antibody, M Gettings for editing the manuscript, and the NIG and VDRC stock centers for RNAi fly strains.

## REFERENCES

1. Laplante M, Sabatini DM. mTOR signaling in growth control and disease. Cell. 2012;149(2):274-93. PubMed PMID: 22500797.
2. Howell JJ, Ricoult SJ, Ben-Sahra I, Manning BD. A growing role for mTOR in promoting anabolic metabolism. Biochem Soc Trans. 2013;41(4):906-12. PubMed PMID: 23863154.
3. Lamming DW, Sabatini DM. A Central role for mTOR in lipid homeostasis. Cell Metab. 2013;18(4):465-9. PubMed PMID: 23973332.
4. Caron A, Richard D, Laplante M. The Roles of mTOR Complexes in Lipid Metabolism. Annu Rev Nutr. 2015;35:321-48. PubMed PMID: 26185979.
5. Shimobayashi M, Hall MN. Making new contacts: the mTOR network in metabolism and signalling crosstalk. Nat Rev Mol Cell Biol. 2014;15(3):155-62. PubMed PMID: 24556838.
6. Saxton RA, Sabatini DM. mTOR Signaling in Growth, Metabolism, and Disease. Cell. 2017;168(6):960-76. doi: 10.1016/j.cell.2017.02.004. PubMed PMID: 28283069; PubMed Central PMCID: PMCPMC5394987.
7. Mossmann D, Park S, Hall MN. mTOR signalling and cellular metabolism are mutual determinants in cancer. Nat Rev Cancer. 2018;18(12):744-57. Epub 2018/11/15. doi: 10.1038/s41568-018-0074-8. PubMed PMID: 30425336.
8. Kim DH, Sarbassov DD, Ali SM, King JE, Latek RR, Erdjument-Bromage H, et al. mTOR interacts with raptor to form a nutrient-sensitive complex that signals to the cell growth machinery. Cell. 2002;110(2):163-75. PubMed PMID: 12150925.
9. Sarbassov DD, Guertin DA, Ali SM, Sabatini DM. Phosphorylation and regulation of Akt/PKB by the rictor-mTOR complex. Science. 2005;307(5712):1098-101. PubMed PMID: 15718470.

509 10. Ugur B, Chen K, Bellen HJ. Drosophila tools and assays for the study of human diseases.
510 Dis Model Mech. 2016;9(3):235-44. doi: 10.1242/dmm.023762. PubMed PMID: 26935102;
511 PubMed Central PMCID: PMCPMC4833332.
512 11. Montagne J, Radimerski T, Thomas G. Insulin signaling: lessons from the Drosophila
513 tuberous sclerosis complex, a tumor suppressor. Sci STKE. 2001;2001(105):PE36.
514 PubMed PMID: 11675514.
515 12. Padmanabha D, Baker KD. Drosophila gains traction as a repurposed tool to investigate
516 metabolism. Trends Endocrinol Metab. 2014;25(10):518-27. doi:
517 10.1016/j.tem.2014.03.011. PubMed PMID: 24768030.
518 13. Antikainen H, Driscoll M, Haspel G, Dobrowolski R. TOR-mediated regulation of
519 metabolism in aging. Aging Cell. 2017;16(6):1219-33. doi: 10.1111/acel.12689. PubMed
520 PMID: 28971552; PubMed Central PMCID: PMCPMC5676073.
521 14. Wangler MF, Hu Y, Shulman JM. Drosophila and genome-wide association studies: a
522 review and resource for the functional dissection of human complex traits. Dis Model Mech.
523 2017;10(2):77-88. doi: 10.1242/dmm.027680. PubMed PMID: 28151408; PubMed Central
524 PMCID: PMCPMC5312009.
525 15. Lehmann M. Endocrine and physiological regulation of neutral fat storage in Drosophila.
526 Mol Cell Endocrinol. 2018;461:165-77. doi: 10.1016/j.mce.2017.09.008. PubMed PMID:
527 28893568; PubMed Central PMCID: PMCPMC5756521.
528 16. Ma XM, Blenis J. Molecular mechanisms of mTOR-mediated translational control. Nat Rev
529 Mol Cell Biol. 2009;10(5):307-18. PubMed PMID: 19339977.
530 17. Goberdhan DC, Ogmundsdottir MH, Kazi S, Reynolds B, Visvalingam SM, Wilson C, et al.
531 Amino acid sensing and mTOR regulation: inside or out? Biochem Soc Trans. 2009;37(Pt
532 1):248-52. PubMed PMID: 19143641.
533 18. Groenewoud MJ, Zwartkruis FJ. Rheb and mammalian target of rapamycin in mitochondrial
534 homoeostasis. Open Biol. 2013;3(12):130185. PubMed PMID: 24352740.
535 19. Dibble CC, Manning BD. Signal integration by mTORC1 coordinates nutrient input with
536 biosynthetic output. Nat Cell Biol. 2013;15(6):555-64. PubMed PMID: 23728461.

20. Montagne J. A Wacky Bridge to mTORC1 Dimerization. Dev Cell. 2016;36(2):129-30. PubMed PMID: 26812011.

21. Yang H, Jiang X, Li B, Yang HJ, Miller M, Yang A, et al. Mechanisms of mTORC1 activation by RHEB and inhibition by PRAS40. Nature. 2017;552(7685):368-73. Epub 2017/12/14. doi: 10.1038/nature25023. PubMed PMID: 29236692; PubMed Central PMCID: PMCPMC5750076.

22. Montagne J, Thomas G. S6K integrates nutrient and mitogen signals to control cell growth. . In: Hall M, Raff, M., Thomas, G., editor. Cell growth: control of cell size. ed: Cold Spring Harbor Press; 2004. p. 265-98.

23. Magnuson B, Ekim B, Fingar DC. Regulation and function of ribosomal protein S6 kinase (S6K) within mTOR signalling networks. Biochem J. 2012;441(1):1-21. PubMed PMID: 22168436.

24. Radimerski T, Montagne J, Hemmings-Mieszczak M, Thomas G. Lethality of Drosophila lacking TSC tumor suppressor function rescued by reducing dS6K signaling. Genes Dev. 2002;16(20):2627-32. PubMed PMID: 12381661.

25. Garami A, Zwartkruis FJ, Nobukuni T, Joaquin M, Roccio M, Stocker H, et al. Insulin activation of Rheb, a mediator of mTOR/S6K/4E-BP signaling, is inhibited by TSC1 and 2. Mol Cell. 2003;11(6):1457-66. PubMed PMID: 12820960.

26. Inoki K, Li Y, Xu T, Guan KL. Rheb GTPase is a direct target of TSC2 GAP activity and regulates mTOR signaling. Genes Dev. 2003;17(15):1829-34. doi: 10.1101/gad.1110003. PubMed PMID: 12869586; PubMed Central PMCID: PMCPMC196227.

27. Dibble CC, Elis W, Menon S, Qin W, Klekota J, Asara JM, et al. TBC1D7 is a third subunit of the TSC1-TSC2 complex upstream of mTORC1. Mol Cell. 2012;47(4):535-46. doi: 10.1016/j.molcel.2012.06.009. PubMed PMID: 22795129; PubMed Central PMCID: PMCPMC3693578.

28. Engelman JA, Luo J, Cantley LC. The evolution of phosphatidylinositol 3-kinases as regulators of growth and metabolism. Nat Rev Genet. 2006;7(8):606-19. doi: 10.1038/nrg1879. PubMed PMID: 16847462.

565 29. Haeusler RA, McGraw TE, Accili D. Biochemical and cellular properties of insulin receptor
566 signalling. Nat Rev Mol Cell Biol. 2018;19(1):31-44. doi: 10.1038/nrm.2017.89. PubMed
567 PMID: 28974775; PubMed Central PMCID: PMCPMC5894887.
568 30. Cully M, You H, Levine AJ, Mak TW. Beyond PTEN mutations: the PI3K pathway as an
569 integrator of multiple inputs during tumorigenesis. Nat Rev Cancer. 2006;6(3):184-92. doi:
570 10.1038/nrc1819. PubMed PMID: 16453012.
571 31. Lien EC, Dibble CC, Toker A. PI3K signaling in cancer: beyond AKT. Curr Opin Cell Biol.
572 2017;45:62-71. doi: 10.1016/j.ceb.2017.02.007. PubMed PMID: 28343126; PubMed Central
573 PMCID: PMCPMC5482768.
574 32. Duvel K, Yecies JL, Menon S, Raman P, Lipovsky AI, Souza AL, et al. Activation of a
575 metabolic gene regulatory network downstream of mTOR complex 1. Mol Cell.
576 2010;39(2):171-83. PubMed PMID: 20670887.
577 33. Polak P, Cybulski N, Feige JN, Auwerx J, Ruegg MA, Hall MN. Adipose-specific knockout
578 of raptor results in lean mice with enhanced mitochondrial respiration. Cell Metab.
579 2008;8(5):399-410. doi: 10.1016/j.cmet.2008.09.003. PubMed PMID: 19046571.
580 34. Peterson TR, Sengupta SS, Harris TE, Carmack AE, Kang SA, Balderas E, et al. mTOR
581 complex 1 regulates lipin 1 localization to control the SREBP pathway. Cell.
582 2011;146(3):408-20. doi: 10.1016/j.cell.2011.06.034. PubMed PMID: 21816276; PubMed
583 Central PMCID: PMCPMC3336367.
584 35. Inoki K, Zhu T, Guan KL. TSC2 mediates cellular energy response to control cell growth
585 and survival. Cell. 2003;115(5):577-90. PubMed PMID: 14651849.
586 36. Choo AY, Kim SG, Vander Heiden MG, Mahoney SJ, Vu H, Yoon SO, et al. Glucose
587 addiction of TSC null cells is caused by failed mTORC1-dependent balancing of metabolic
588 demand with supply. Mol Cell. 2010;38(4):487-99. doi: 10.1016/j.molcel.2010.05.007.
589 PubMed PMID: 20513425; PubMed Central PMCID: PMCPMC2896794.
590 37. Csibi A, Lee G, Yoon SO, Tong H, Ilter D, Elia I, et al. The mTORC1/S6K1 pathway
591 regulates glutamine metabolism through the eIF4B-dependent control of c-Myc translation.

592 Curr Biol. 2014;24(19):2274-80. doi: 10.1016/j.cub.2014.08.007. PubMed PMID: 25220053;
593 PubMed Central PMCID: PMCPMC4190129.
594 38. Csibi A, Fendt SM, Li C, Poulogiannis G, Choo AY, Chapski DJ, et al. The mTORC1
595 pathway stimulates glutamine metabolism and cell proliferation by repressing SIRT4. Cell.
596 2013;153(4):840-54. doi: 10.1016/j.cell.2013.04.023. PubMed PMID: 23663782; PubMed
597 Central PMCID: PMCPMC3684628.
598 39. Hahn-Windgassen A, Nogueira V, Chen CC, Skeen JE, Sonenberg N, Hay N. Akt activates
599 the mammalian target of rapamycin by regulating cellular ATP level and AMPK activity. J
600 Biol Chem. 2005;280(37):32081-9. doi: 10.1074/jbc.M502876200. PubMed PMID:
601 16027121.
602 40. Robey RB, Hay N. Is Akt the "Warburg kinase"?-Akt-energy metabolism interactions and
603 oncogenesis. Semin Cancer Biol. 2009;19(1):25-31. doi: 10.1016/j.semcancer.2008.11.010.
604 PubMed PMID: 19130886; PubMed Central PMCID: PMCPMC2814453.
605 41. Jaldin-Fincati JR, Pavarotti M, Frendo-Cumbo S, Bilan PJ, Klip A. Update on GLUT4
606 Vesicle Traffic: A Cornerstone of Insulin Action. Trends Endocrinol Metab. 2017;28(8):597-
607 611. doi: 10.1016/j.tem.2017.05.002. PubMed PMID: 28602209.
608 42. Gottlob K, Majewski N, Kennedy S, Kandel E, Robey RB, Hay N. Inhibition of early
609 apoptotic events by Akt/PKB is dependent on the first committed step of glycolysis and
610 mitochondrial hexokinase. Genes Dev. 2001;15(11):1406-18. doi: 10.1101/gad.889901.
611 PubMed PMID: 11390360; PubMed Central PMCID: PMCPMC312709.
612 43. Houddane A, Bultot L, Novellasdemunt L, Johanns M, Gueuning MA, Vertommen D, et al.
613 Role of Akt/PKB and PFKFB isoenzymes in the control of glycolysis, cell proliferation and
614 protein synthesis in mitogen-stimulated thymocytes. Cell Signal. 2017;34:23-37. doi:
615 10.1016/j.cellsig.2017.02.019. PubMed PMID: 28235572.
616 44. Nakae J, Kitamura T, Silver DL, Accili D. The forkhead transcription factor Foxo1 (Fkhr)
617 confers insulin sensitivity onto glucose-6-phosphatase expression. J Clin Invest.
618 2001;108(9):1359-67. doi: 10.1172/JCI12876. PubMed PMID: 11696581; PubMed Central
619 PMCID: PMCPMC209440.

620 45. McManus EJ, Sakamoto K, Armit LJ, Ronaldson L, Shpiro N, Marquez R, et al. Role that
621 phosphorylation of GSK3 plays in insulin and Wnt signalling defined by knockin analysis.
622 EMBO J. 2005;24(8):1571-83. doi: 10.1038/sj.emboj.7600633. PubMed PMID: 15791206;
623 PubMed Central PMCID: PMCPMC1142569.
624 46. Majewski N, Nogueira V, Bhaskar P, Coy PE, Skeen JE, Gottlob K, et al. Hexokinase-
625 mitochondria interaction mediated by Akt is required to inhibit apoptosis in the presence or
626 absence of Bax and Bak. Mol Cell. 2004;16(5):819-30. doi: 10.1016/j.molcel.2004.11.014.
627 PubMed PMID: 15574336.
628 47. Hagiwara A, Cornu M, Cybulski N, Polak P, Betz C, Trapani F, et al. Hepatic mTORC2
629 activates glycolysis and lipogenesis through Akt, glucokinase, and SREBP1c. Cell Metab.
630 2012;15(5):725-38. doi: 10.1016/j.cmet.2012.03.015. PubMed PMID: 22521878.
631 48. Yuan M, Pino E, Wu L, Kacergis M, Soukas AA. Identification of Akt-independent regulation
632 of hepatic lipogenesis by mammalian target of rapamycin (mTOR) complex 2. J Biol Chem.
633 2012;287(35):29579-88. doi: 10.1074/jbc.M112.386854. PubMed PMID: 22773877;
634 PubMed Central PMCID: PMCPMC3436168.
635 49. Radimerski T, Montagne J, Rintelen F, Stocker H, van der Kaay J, Downes CP, et al. dS6K-
636 regulated cell growth is dPKB/dPI(3)K-independent, but requires dPDK1. Nat Cell Biol.
637 2002;4(3):251-5. PubMed PMID: 11862217.
638 50. Dong J, Pan D. Tsc2 is not a critical target of Akt during normal Drosophila development.
639 Genes Dev. 2004;18(20):2479-84. PubMed PMID: 15466161.
640 51. Montagne J, Lecerf C, Parvy JP, Bennion JM, Radimerski T, Ruhf ML, et al. The nuclear
641 receptor DHR3 modulates dS6 kinase-dependent growth in Drosophila. PLoS Genet.
642 2010;6:e1000937. PubMed PMID: 20463884.
643 52. Pallares-Cartes C, Cakan-Akdogan G, Teleman AA. Tissue-specific coupling between
644 insulin/IGF and TORC1 signaling via PRAS40 in Drosophila. Dev Cell. 2012;22(1):172-82.
645 doi: 10.1016/j.devcel.2011.10.029. PubMed PMID: 22264732.

646 53. Stocker H, Radimerski T, Schindelholz B, Wittwer F, Belawat P, Daram P, et al. Rheb is an
647 essential regulator of S6K in controlling cell growth in Drosophila. Nat Cell Biol.
648 2003;5(6):559-65. PubMed PMID: 12766775.
649 54. Oldham S, Montagne J, Radimerski T, Thomas G, Hafen E. Genetic and biochemical
650 characterization of dTOR, the Drosophila homolog of the target of rapamycin. Genes Dev.
651 2000;14(21):2689-94. PubMed PMID: 11069885.
652 55. Edgar BA, Orr-Weaver TL. Endoreplication cell cycles: more for less. Cell.
653 2001;105(3):297-306. PubMed PMID: 11348589.
654 56. Zhang H, Stallock JP, Ng JC, Reinhard C, Neufeld TP. Regulation of cellular growth by the
655 Drosophila target of rapamycin dTOR. Genes Dev. 2000;14(21):2712-24. PubMed PMID:
656 11069888.
657 57. Morata G, Ripoll P. Minutes: mutants of drosophila autonomously affecting cell division rate.
658 Dev Biol. 1975;42(2):211-21. PubMed PMID: 1116643.
659 58. Romero-Pozuelo J, Demetriades C, Schroeder P, Teleman AA. CycD/Cdk4 and
660 Discontinuities in Dpp Signaling Activate TORC1 in the Drosophila Wing Disc. Dev Cell.
661 2017;42(4):376-87 e5. doi: 10.1016/j.devcel.2017.07.019. PubMed PMID: 28829945.
662 59. Garrido D, Rubin T, Poidevin M, Maroni B, Le Rouzic A, Parvy JP, et al. Fatty Acid
663 Synthase Cooperates with Glyoxalase 1 to Protect against Sugar Toxicity. PLoS Genet.
664 2015;11(2):e1004995. PubMed PMID: 25692475.
665 60. Parvy JP, Napal L, Rubin T, Poidevin M, Perrin L, Wicker-Thomas C, et al. Drosophila
666 melanogaster Acetyl-CoA-carboxylase sustains a fatty acid-dependent remote signal to
667 waterproof the respiratory system. PLoS Genet. 2012;8(8):e1002925. PubMed PMID:
668 22956916.
669 61. Chung H, Loehlin DW, Dufour HD, Vaccarro K, Millar JG, Carroll SB. A single gene affects
670 both ecological divergence and mate choice in Drosophila. Science. 2014;343(6175):1148-
671 51. PubMed PMID: 24526311.

672 62. Wicker-Thomas C, Garrido D, Bontonou G, Napal L, Mazuras N, Denis B, et al. Flexible
673 origin of hydrocarbon/pheromone precursors in Drosophila melanogaster. J Lipid Res.
674 2015;56(11):2094-101. PubMed PMID: 26353752.
675 63. Parvy JP, Wang P, Garrido D, Maria A, Blais C, Poidevin M, et al. Forward and feedback
676 regulation of cyclic steroid production in Drosophila melanogaster. Development.
677 2014;141(20):3955-65. PubMed PMID: 25252945.
678 64. Montagne J, Stewart MJ, Stocker H, Hafen E, Kozma SC, Thomas G. Drosophila S6
679 kinase: a regulator of cell size. Science. 1999;285(5436):2126-9. PubMed PMID:
680 10497130.
681 65. Rulifson EJ, Kim SK, Nusse R. Ablation of insulin-producing neurons in flies: growth and
682 diabetic phenotypes. Science. 2002;296(5570):1118-20. PubMed PMID: 12004130.
683 66. Mattila J, Havula E, Suominen E, Teesalu M, Surakka I, Hynynen R, et al. Mondo-Mlx
684 Mediates Organismal Sugar Sensing through the Gli-Similar Transcription Factor
685 Sugarbabe. Cell Rep. 2015;13(2):350-64. PubMed PMID: 26440885.
686 67. Richards P, Ourabah S, Montagne J, Burnol AF, Postic C, Guilmeau S. MondoA/ChREBP:
687 The usual suspects of transcriptional glucose sensing; Implication in pathophysiology.
688 Metabolism. 2017;70:133-51. doi: 10.1016/j.metabol.2017.01.033. PubMed PMID:
689 28403938.
690 68. Sassu ED, McDermott JE, Keys BJ, Esmaeili M, Keene AC, Birnbaum MJ, et al.
691 Mio/dChREBP coordinately increases fat mass by regulating lipid synthesis and feeding
692 behavior in Drosophila. Biochem Biophys Res Commun. 2012;426(1):43-8. doi:
693 10.1016/j.bbrc.2012.08.028. PubMed PMID: 22910416; PubMed Central PMCID:
694 PMCPMC3445662.
695 69. Bruning U, Morales-Rodriguez F, Kalucka J, Goveia J, Taverna F, Queiroz KCS, et al.
696 Impairment of Angiogenesis by Fatty Acid Synthase Inhibition Involves mTOR Malonylation.
697 Cell Metab. 2018;28(6):866-80 e15. Epub 2018/08/28. doi: 10.1016/j.cmet.2018.07.019.
698 PubMed PMID: 30146486.

699 70. Caldwell PE, Walkiewicz M, Stern M. Ras activity in the Drosophila prothoracic gland
700 regulates body size and developmental rate via ecdysone release. Curr Biol.
701 2005;15(20):1785-95. PubMed PMID: 16182526.
702 71. Colombani J, Bianchini L, Layalle S, Pondeville E, Dauphin-Villemant C, Antoniewski C, et
703 al. Antagonistic actions of ecdysone and insulins determine final size in Drosophila.
704 Science. 2005;310(5748):667-70. PubMed PMID: 16179433.
705 72. Mirth C. Ecdysteroid control of metamorphosis in the differentiating adult leg structures of
706 Drosophila melanogaster. Dev Biol. 2005;278(1):163-74. PubMed PMID: 15649469.
707 73. Wipperman MF, Montrose DC, Gotto AM, Jr., Hajjar DP. Mammalian Target of Rapamycin:
708 A Metabolic Rheostat for Regulating Adipose Tissue Function and Cardiovascular Health.
709 Am J Pathol. 2019;189(3):492-501. Epub 2019/02/26. doi: 10.1016/j.ajpath.2018.11.013.
710 PubMed PMID: 30803496.
711 74. Harachi M, Masui K, Okamura Y, Tsukui R, Mischel PS, Shibata N. mTOR Complexes as a
712 Nutrient Sensor for Driving Cancer Progression. Int J Mol Sci. 2018;19(10). Epub
713 2018/10/24. doi: 10.3390/ijms19103267. PubMed PMID: 30347859.
714 75. Tian T, Li X, Zhang J. mTOR Signaling in Cancer and mTOR Inhibitors in Solid Tumor
715 Targeting Therapy. Int J Mol Sci. 2019;20(3). Epub 2019/02/14. doi: 10.3390/ijms20030755.
716 PubMed PMID: 30754640; PubMed Central PMCID: PMCPMC6387042.
717 76. Henske EP, Jozwiak S, Kingswood JC, Sampson JR, Thiele EA. Tuberous sclerosis
718 complex. Nat Rev Dis Primers. 2016;2:16035. doi: 10.1038/nrdp.2016.35. PubMed PMID:
719 27226234.
720 77. Guri Y, Colombi M, Dazert E, Hindupur SK, Roszik J, Moes S, et al. mTORC2 Promotes
721 Tumorigenesis via Lipid Synthesis. Cancer Cell. 2017;32(6):807-23 e12. doi:
722 10.1016/j.ccell.2017.11.011. PubMed PMID: 29232555.
723 78. Dietzl G, Chen D, Schnorrer F, Su KC, Barinova Y, Fellner M, et al. A genome-wide
724 transgenic RNAi library for conditional gene inactivation in Drosophila. Nature.
725 2007;448(7150):151-6. PubMed PMID: 17625558.

79. Bohni R, Riesgo-Escovar J, Oldham S, Brogiolo W, Stocker H, Andruss BF, et al. Autonomous control of cell and organ size by CHICO, a Drosophila homolog of vertebrate IRS1-4. Cell. 1999;97(7):865-75. PubMed PMID: 10399915.

80. Lee T, Luo L. Mosaic analysis with a repressible cell marker (MARCM) for Drosophila neural development. Trends Neurosci. 2001;24(5):251-4. PubMed PMID: 11311363.

81. Holm S. A simple sequentially rejective multiple test procedure. Scand J Statist. 1079;6(65-70).

82. Hothorn T, Bretz F, Westfall P. Simultaneous inference in general parametric models. Biom J. 2008;50(3):346-63. Epub 2008/05/16. doi: 10.1002/bimj.200810425. PubMed PMID: 18481363.

83. Bates D, Mächler M, Bolker BM, Walker S. Fitting Linear Mixed-Effects Models Using lme4. Journal of Statistical Software. 2015;67(1):1-48. doi: 10.18637/jss.v067.i01.

## FIGURE LEGENDS

**Figure 1: mTORC1 and mTORC2 dependent growth in FB cells.** (**A-L**) MARCM clones labeled by GFP (green) in the FB of L3 larvae. Nuclei were labeled with DAPI (silver) and membranes with phalloidin (red). Control (A), *Rheb*$^{+}$ (B), *PTEN*$^{-/-}$ (C) and *PTEN*$^{-/-}$;*Rheb*$^{+}$ (D) clones were generated in a wild type background. *Rheb*$^{+}$ (E), *PTEN*$^{-/-}$ (F), *mTOR*$^{2L1}$ (G) *mTOR*$^{2L1}$, *Rheb*$^{+}$ (H) *mTOR*$^{2L1}$,*PTEN*$^{-/-}$ (I), *mTOR*$^{\Delta P}$ (J), *mTOR*$^{\Delta P}$,*Rheb*$^{+}$ (K) and *mTOR*$^{\Delta P}$,*PTEN*$^{-/-}$ (L) clones were generated in a *Minute* (*M*) background. Scale bars: 50µm. (**M**) Relative size of control (Co), *Rheb*$^{+}$, *PTEN*$^{-/-}$, and *PTEN*$^{-/-}$;*Rheb*$^{+}$ clonal cells generated in a wild type background.

**Figure 2: mTORC1 and mTORC2 activity in FB cells.** (**A-J**) MARCM clones labeled by GFP (green) in the FB of L3 larvae. Clones were generated in a wild type (A,D,E,H,I,J) or a *Minute* (B,C,F,G) background and nuclei were labeled with DAPI (silver). FB tissues with *PTEN*$^{-/-}$ (A),

752 *mTOR$^{\Delta P}$* (B), *mTOR$^{2L1}$* (C) and *FASN$^{1-2}$* (J) clones were stained with a phospho-AKT antibody.
753 FB tissues with control (D), *mTOR$^{\Delta P}$* (E), *mTOR$^{2L1}$* (F) *Rheb$^{+}$* (G), *PTEN$^{-/-}$* (H) and *FASN$^{1-2}$* (I)
754 clones were stained with a phospho-S6 antibody. Scale bars: 50µm. (**K**) Percentage of P-S6
755 positive clones with respect to the total number of MARCM clones for control, *FASN$^{1-2}$*, *PTEN$^{-/-}$*,
756 *Rheb$^{+}$*, *mTOR$^{2L1}$* and *mTOR$^{\Delta P}$* genotypes.

757

758 **Figure 3: Enhanced mTORC1 or mTORC2 signaling affects larval metabolism.** (**A-B**) Body
759 weight of female (A) and male (B) prepupae formed from larvae fed either a standard (0%) or a
760 20%-SSD (20%) as from the L2/L3 transition. (**C-F**) Measurement of total protein (C), TAG (D),
761 glycogen (E) and trehalose (F) levels in prepupae fed either a standard or a 20%-SSD.
762 Prepupae used in these measurements were the F1 progeny from *da-gal4* virgin females mated
763 to either control (Co), *EP(UAS)-Rheb* (*Rheb$^{++}$*) or *UAS-PTEN-RNAi* (*PTEN-Ri*) males.

764

765 **Figure 4: Glycolysis knockdown in whole organisms.** (**A**) Scheme of basal metabolism.
766 Glucose and trehalose enter glycolysis as glucose-6P, whereas fructose follows a distinct
767 pathway to triose-P. Enzymes investigated in the present study are marked in red. (**B**)
768 Phenotype of ubiquitous RNAi knockdown of PFK1, PK, LDH and PDH. Flies were left to lay
769 eggs overnight either at 29°C (column 0h) or at 19°C and transferred to 29°C the day after
770 (column 24h); then development proceeded at 29°C (i.e. the temperature that inactivates
771 Gal80). (**C**) Western-blot analysis of total (top) or phosphorylated (mid) dS6K (left) or Akt (right)
772 proteins; tubulin (bottom) was used as a loading control. Protein extracts were prepared with
773 late L2 control larvae (Co) or L2 larvae expressing RNAi against the indicated metabolic
774 enzymes. (**E-F**) Survival at 29°C of male (top) and female (bottom) control flies or flies
775 expressing RNAi against the indicated metabolic enzymes as from adult eclosion.

776

**Figure 5: Cell-autonomous requirement of glycolytic enzymes for mTOR-dependent overgrowth.** (**A-G**) MARCM clones labeled by GFP (green) in the FB of L3 larvae. Nuclei were labeled with DAPI (silver) and membranes with phalloidin (red). Genotypes of MARCM clones are: *PFK1-RNAi* (A), *PK-RNAi* (B), *LDH-RNAi* (C), *PDH-RNAi* (D), *Rheb*$^{+}$,*PFK1-RNAi* (E), *Rheb*$^{+}$,*PK-RNAi* (F), *Rheb*$^{+}$,*LDH-RNAi* (G), *Rheb*$^{+}$,*PDH-RNAi* (H), *PTEN*$^{-/-}$;*PFK1-RNAi* (I), *PTEN*$^{-/-}$;*PK-RNAi* (J), *PTEN*$^{-/-}$;*PDH-RNAi* (K) and *PTEN*$^{-/-}$;*PDH-RNAi* (L). Scale bars: 50µm. (**M**) Relative size of clonal cells corresponding to the clones shown in A-L, and in Figure 2A for control (Co).

**Figure 6: *FASN*$^{1-2}$ mutation affects developmental growth and mTOR signaling.** (**A**) Developmental duration from egg laying to metamorphosis onset of *w*$^{1118}$ control (Co) and *FASN*$^{1-2}$ (FASN) larvae fed either a beySD (0%) or a 10% sucrose-supplemented-beySD as from the L2/L3 transition (10%); n: total number of larvae collected for each condition. (**B**) Prepupal weight of females (left) and males (right) as listed in 4A; the numbers of weighted prepupae are indicated above each sample. (**C**) Western-blot analysis of (from top to bottom) total dS6K, phosphorylated dS6K, total Akt, phosphorylated Akt and total tubulin as a loading control. Protein extracts were prepared from feeding L3 larvae prior to the wandering stage as listed in 4A. For each condition, at least 30 larvae were used to prepare protein extracts.

**Figure 7: Cell-autonomous requirement of FASN activity for mTOR-dependent overgrowth.** (**A-L**) MARCM clones labeled by GFP (green) in the FB of L3 larvae fed either a standard (A-C, G-I) or a 20%-SSD (D-E, J-L). Nuclei were labeled with DAPI (silver) and membranes with phalloidin (red). Genotypes of MARCM clones are: *Rheb*$^{+}$ (A,D), *PTEN*$^{-/-}$ (B,E) *PTEN*$^{-/-}$,*Rheb*$^{+}$ (C,F), *FASN*$^{1-2}$;*Rheb*$^{+}$ (G,J) *FASN*$^{1-2}$,*PTEN*$^{-/-}$ (H,K) and the *FASN*$^{1-2}$,*PTEN*$^{-/-}$;*Rheb*$^{+}$ (I,L). Scale bars: 50µm. (**M**) Relative size of clonal cells corresponding to the clones shown in A-L and in supplementary Fig S1 for *FASN*$^{1-2}$ and Figure 1A for control (Co).

803

804 **SUPPORTING INFORMATIONS**

805 **S1 Table. Statistical tests corresponding to figures 1M (A), 5M (B), and 7M (C).** The model
806 tests for the difference is the log ratio of *GFP⁺/GFP⁻surrounding* cells between pairs of
807 genotypes (Co = control), accounting for larvae and series random effects (see the Methods
808 section). P-values were corrected for multiple testing (Holm-Bonferroni method) and quantify the
809 risk of rejecting the true null hypothesis at the table level.

810

811 **S2 Table. Statistical test of the difference in frequency between MARCM clones to**
812 **control.** The model is a mixed effect, generalized linear model considering frequencies as
813 binomial data and genotype as a fixed effect, while larvae / series were random effects. P-
814 values were adjusted for multiple testing by a Holm-Bonferroni correction.

815

816 **S3 Table. Statistical tests corresponding to Figure 3.** Differences in male (A) or female (B)
817 weight, in protein (C), in TAG (D), in glycogen (E) and in trehalose (F) between control (Co) and
818 prepupae that ubiquitously express either Rheb (*Rheb⁺⁺*) or an RNAi to PTEN (*PTENi*). The
819 column at the right indicates P-values corrected for multiple testing (Holm-Bonferoni correction).

820

821 **S4 Table. Statistical tests corresponding to Figure 6B.** Prepupal weight differences in males
822 and females (Estimate and standard error, in mg) between control (*w⁻*) and *FASN¹⁻²* animals fed
823 either a standard (0%) or a sucrose enriched diet (10%). The **Pr** column (right) indicates P-
824 values corrected for multiple testing (Holm-Bonferoni correction).

825

826 **S1 Fig. Effect of dietary sugar on *FASN*$^{1-2}$ mutant cells.** *FASN*$^{1-2}$ MARCM clones labeled by
827 GFP (green) in the FB of L3 larvae fed either a standard (A) or a 20%-SSD (B). Nuclei are
828 labeled with DAPI (silver) and membranes by phalloidin (red). Scale bars: 50μm.

829

830 **S2 Fig. Knockdown efficacy of the RNAi to the glycolytic enzymes.** (**A**) mRNA expression
831 in control larvae (blue bars, +/- standard error) was adjusted to 100. mRNA levels after RNAi
832 knockdown (red bars, +/- standard error) was calculated as a percentage of corresponding
833 expression in control larvae. (**B**) Oligonucleotides used in RT-Q-PCR for each glycolytic
834 enzyme.

835

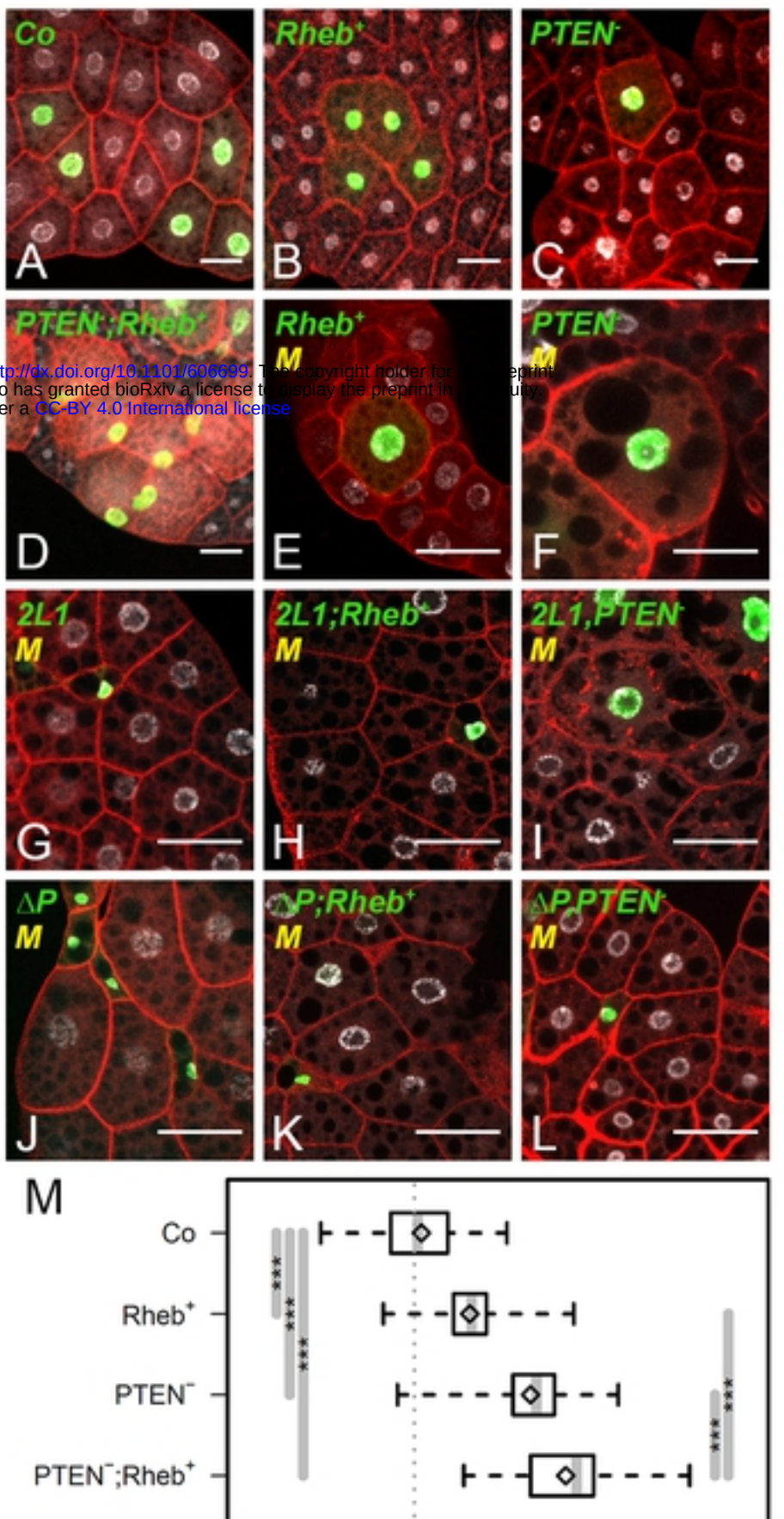


Figure 1

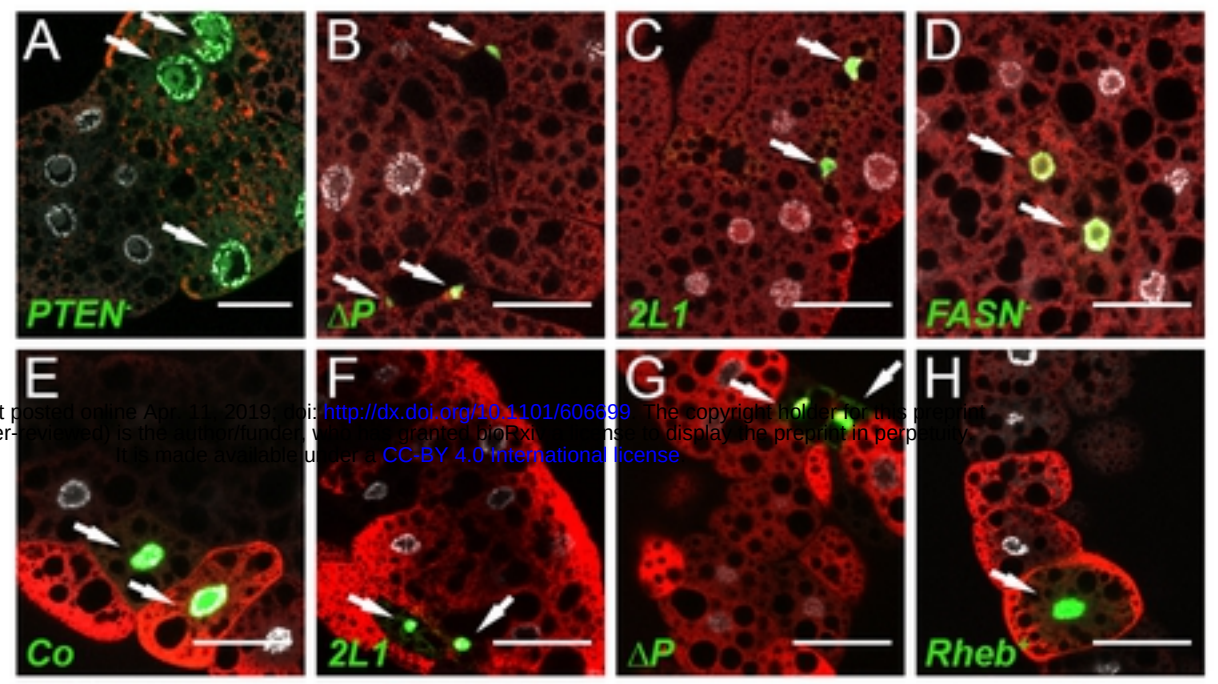


Figure 2

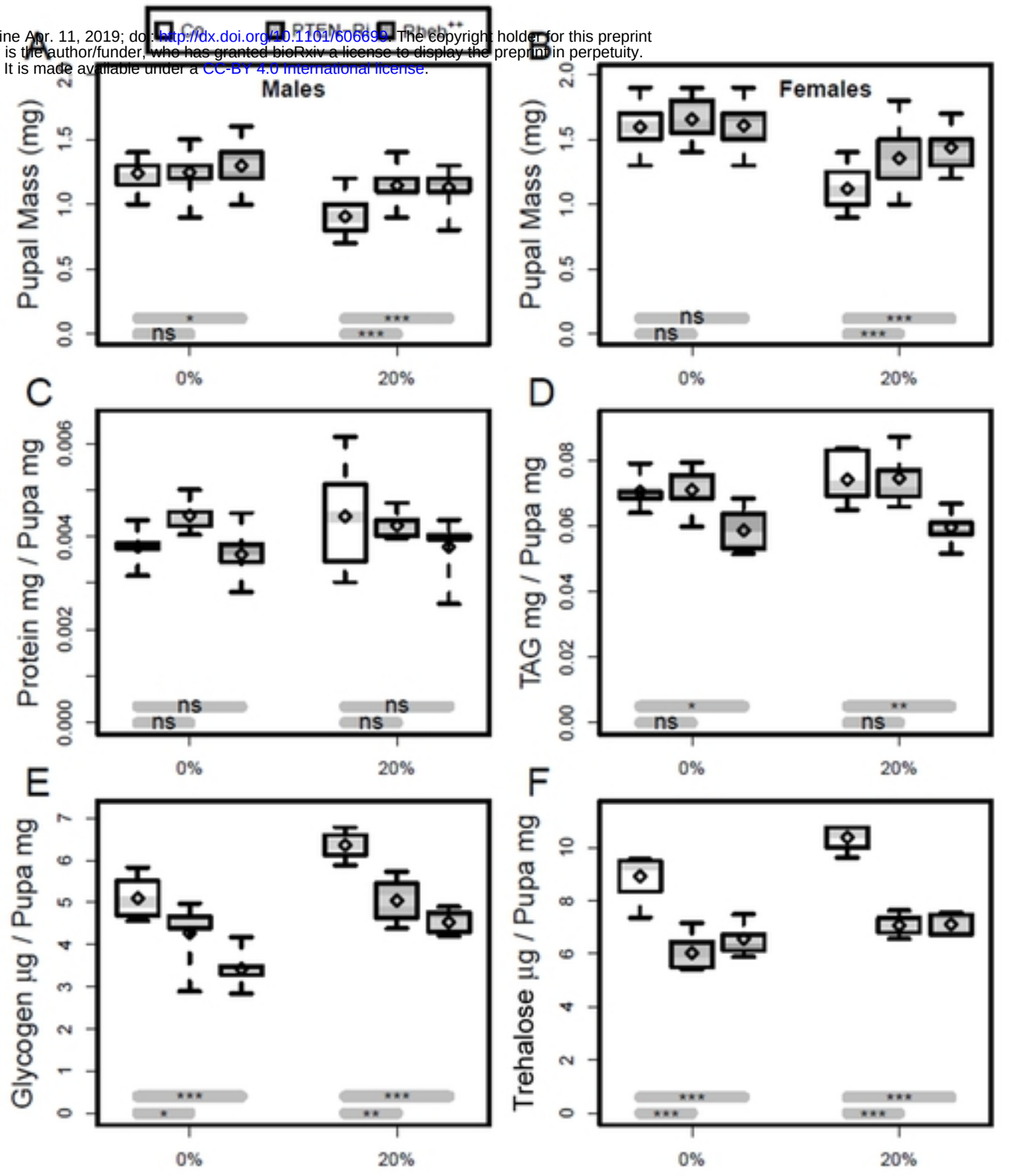


Figure 3

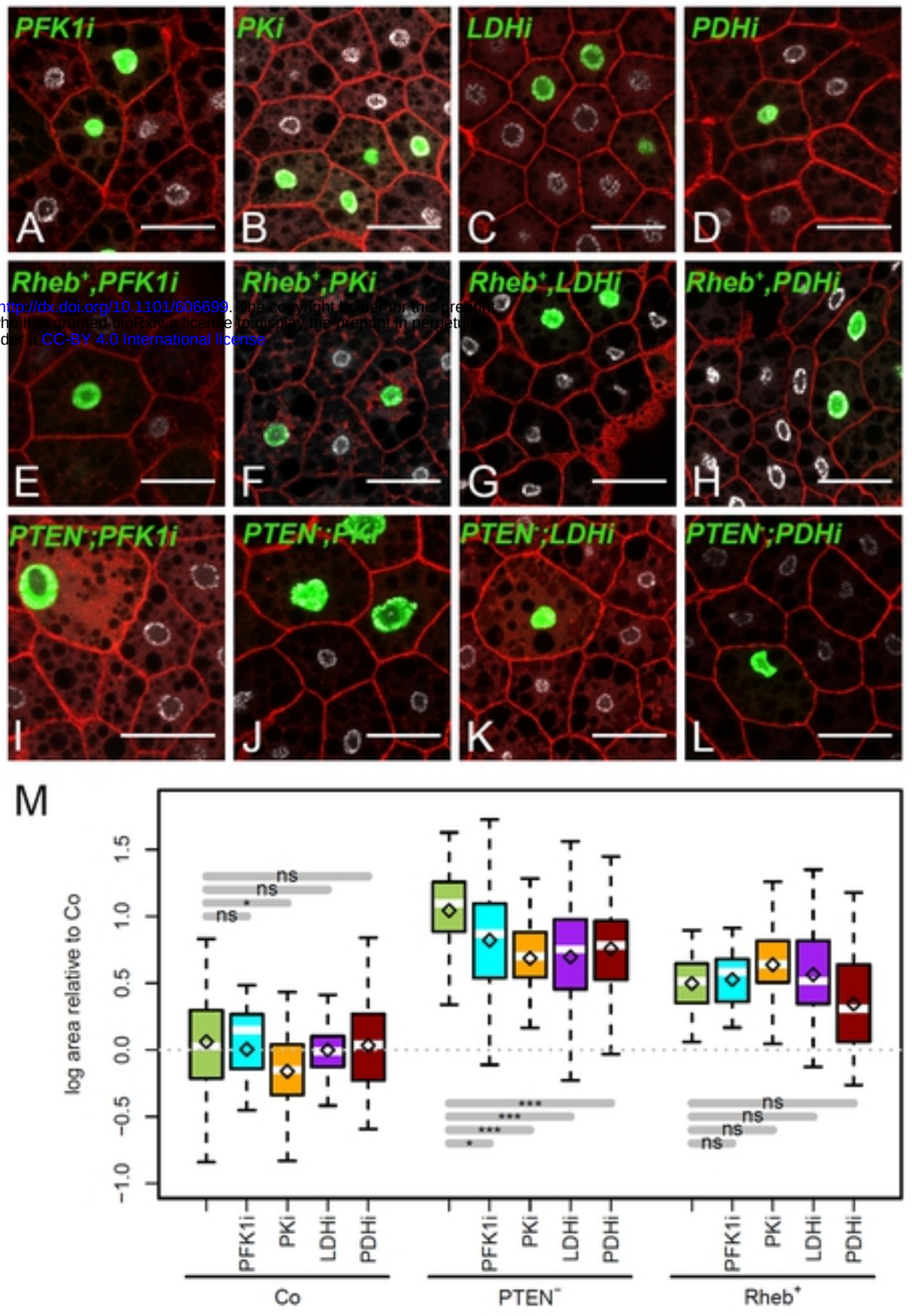


Figure 5

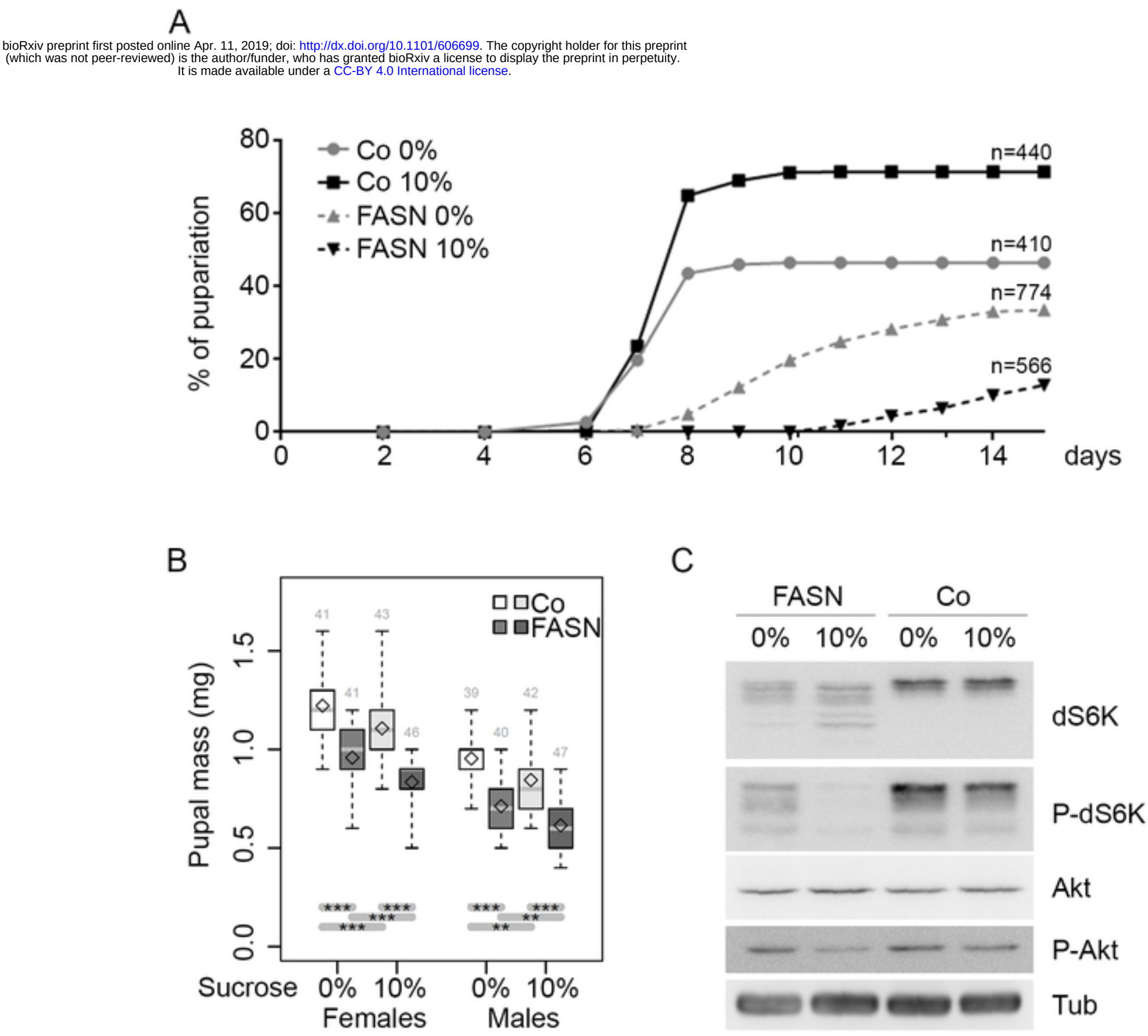


Figure 6

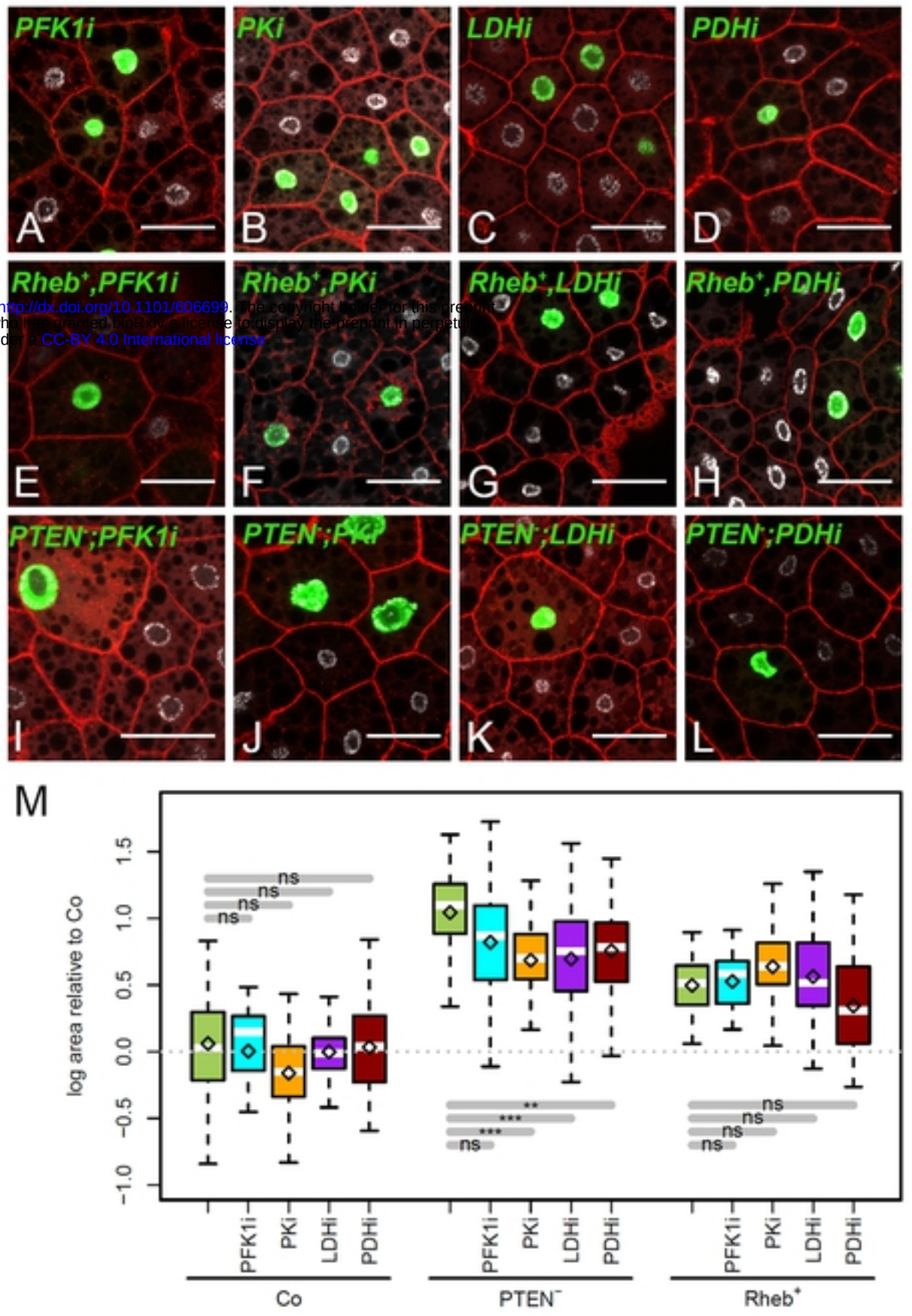


Figure 7

A

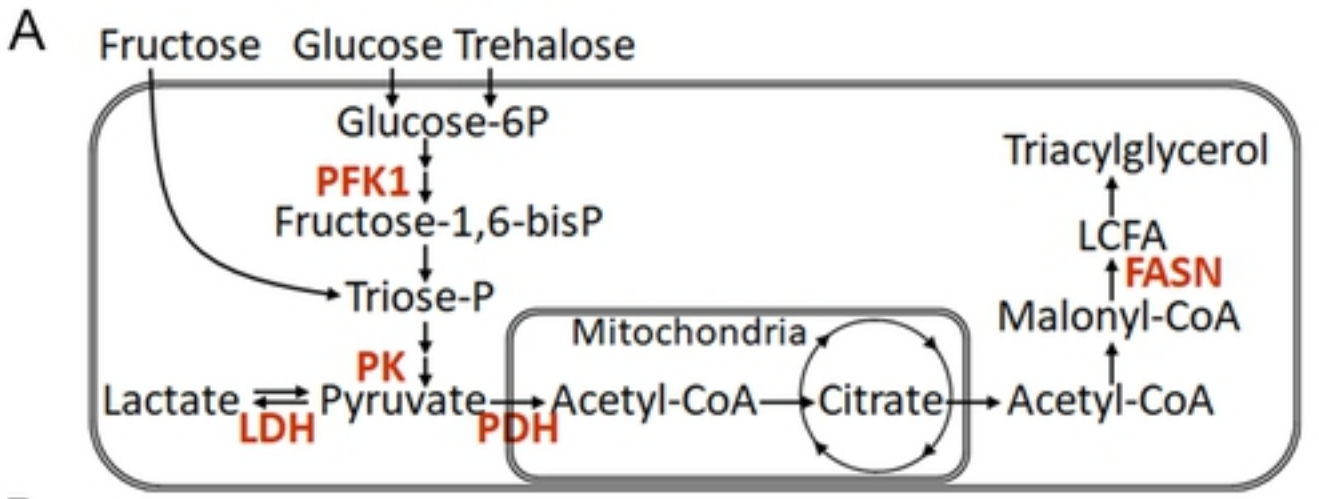


B

| 19°C>>29°C | 0h | 24h |
|---|---|---|
| PFK1-Ri | † L1/L2 | † late L2 |
| PK-Ri | † L2/L3 | † L3/pp |
| LDH-Ri | † L2/L3 | † L3/pp |
| PDH-Ri | ½† L3/pp | ½† L3/pp |

C

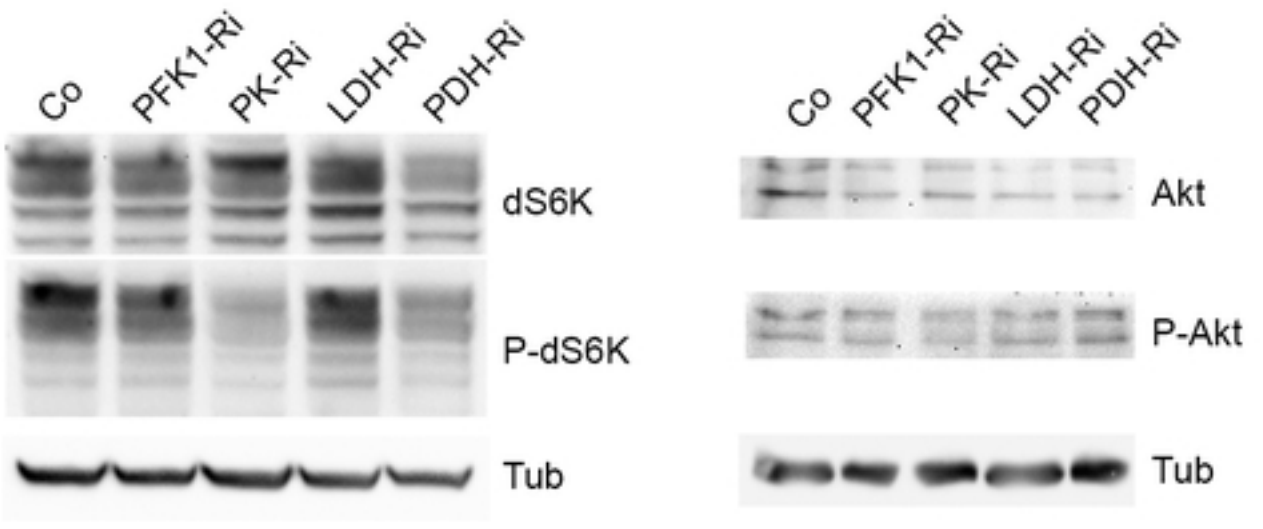


D

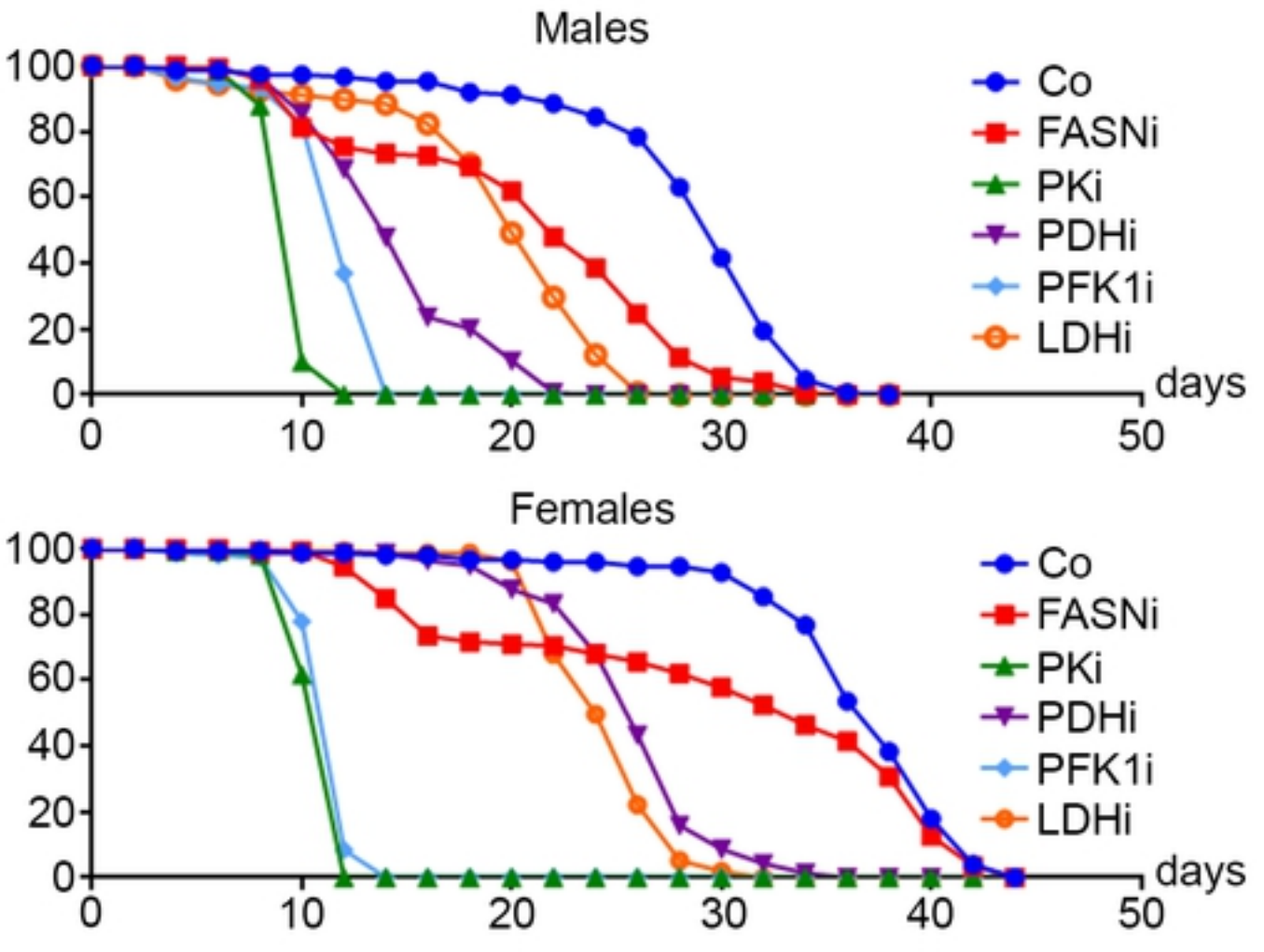


Figure 4